IMA Journal of Numerical Analysis (2014) **34**, 759–781
doi:10.1093/imanum/drt018
Advance Access publication on July 17, 2013

A virtual element method with arbitrary regularity

Lourenco Beirão da Veiga
Dipartimento di Matematica F. Enriques, Università degli Studi di Milano, via Saldini 50, 20133 Milano, Italy
lourenco.beirao@unimi.it

and

Gianmarco Manzini*
Los Alamos National Laboratory, Plasma Physics and Applied Mathematics Group, T-5, Theoretical Division, MS B284, Los Alamos, NM 87544, USA and Centro di Simulazione Numerica Avanzata (CeSNA)–IUSS Pavia, v.le Lungo Ticino Sforza 56, I - 27100 Pavia, Italy and Istituto di Matematica Applicata e Tecnologie Informatiche (IMATI) – CNR, via Ferrata 1, I - 27100 Pavia, Italy
*Corresponding author: marco.manzini@imati.cnr.it gmanzini@lanl.gov

[Received on 6 September 2012; revised on 27 January 2013]

We develop and analyse a new family of virtual element methods on unstructured polygonal meshes for the diffusion problem in primal form, which uses arbitrarily regular discrete spaces $V_h \subset C^\alpha$, $\alpha \in \mathbb{N}$. The degrees of freedom are (a) solution and derivative values of various degrees at suitable nodes and (b) solution moments inside polygons. The convergence of the method is proved theoretically and an optimal error estimate is derived. Numerical experiments confirm the convergence rate that is expected from the theory.

Keywords: diffusion problem; virtual element method; polygonal mesh; high-order scheme; mimetic finite difference method; Galerkin method.

1. Introduction

In this work, we investigate a very appealing feature of the virtual element method (VEM): the design of numerical schemes that incorporate a given degree $\alpha \in \mathbb{N}$ of C^α global regularity into the discrete solution. Indeed, the discrete spaces of the conforming finite element method are traditionally globally continuous, that is, only C^0, and the construction of more regular elements, for example, C^1 elements, is a very difficult task. Successful C^1 discretizations date back to the mid sixties to early seventies and were obtained by using either a high polynomial degree, as, for example, in the *Argyris and Bell* triangle (Argyris *et al.*, 1968; Bell, 1969; Ciarlet, 1978), or a complex design, as, for example, the Hsieh-Clough-Tocher (HCT) triangle (Clough & Tocher, 1965; Ciarlet, 1978). Moreover, using such strategies to obtain a finite element space with C^2 or higher regularity becomes prohibitive. To the authors knowledge, the only technology that succeeded later on in building piecewise polynomial and highly regular spaces is that of splines (de Boor, 2001; Schumaker, 2007) and isogeometric analysis (Cottrell *et al.*, 2009), but at the cost of using tensor-product meshes or resorting to the much more complex construction of *T-splines*.

The virtual element approach in Beirão da Veiga *et al.* (2013,?) offers a strong alternative to such constructions: the finite element spaces that we will consider in this work are *virtual* in the sense that we do not need to build the basis functions explicitly to implement the method. This feature allows

us to design a family of numerical methods that are associated with discrete spaces with arbitrary C^α regularity and are suitable for general unstructured polygonal meshes. To this end, we propose a new VEM that depends on two integer parameters: α for the regularity and m for the polynomial degree of the approximation, with the minimal condition that $m \geqslant \alpha + 1$. The parameter α determines the global smoothness of the underlying discrete space, that is, C^α regularity across the edges of the mesh. The parameter m determines the order of convergence of the method in the energy norm, which is expected to be $\mathcal{O}(h^m)$ for a sufficiently regular solution.

Although the present paper is complete, we intend this contribution as a first step in exploring a new direction. Indeed, the possibility of developing highly regular methods could pave the way to a wide range of applications. At first glance, the main advantages offered by the VEM lie in simpler discretization of higher-order problems (see, for example, Brezzi & Marini, 2013) and in the straightforward computation of derived quantities such as fluxes, strains, stresses, etc., which are directly related to the degrees of freedom of the numerical method. New research topics could also be anisotropic error estimation based on the Hessian of the solution and the construction of finite element spaces that exactly satisfy given constraints, as, for example, in the stream function formulation of the Stokes problem, where the discrete velocity is the curl of a C^1 scalar field. We can also devise a VEM for better eigenvalue approximation, as studies in isogeometric analysis have shown that highly regular discrete spaces may give a better approximation of the high end of the spectrum. Finally, the present construction can be extended to a more general approach in which the polynomial degree may vary from element to element and the regularity index α may vary from edge to edge.

These goals may be achieved while still keeping the property of mesh generality of mimetic finite difference (MFD) methods; see, for example, the mixed and primal formulations given in Brezzi *et al.* (2005a, 2009) and Beirão da Veiga *et al.* (2011b). The VEM can, indeed, be considered as a Galerkin reformulation of the MFD method. This fact is of primary importance since it establishes a clear and well-defined bridge between MFD methods and the finite element framework. Such reformulations for mixed and nodal MFD methods allow us to extend mimetic technology (see, for example, Brezzi *et al.*, 2005a,b, 2009; Beirão da Veiga, 2008, 2010; Beirão da Veiga & Manzini, 2008; Cangiani & Manzini, 2008; Beirão da Veiga *et al.*, 2009a,b, 2011b; Cangiani *et al.*, 2009; Lipnikov *et al.*, 2011) to the VEM. Other approaches that generalize finite element methods to elements of general shape are found, for instance, in Belytschko *et al.* (1994), Benson *et al.* (2010), Cueto *et al.* (2003), Fries & Belytschko (2010), Mousavi & Sukumar (2011), Sukumar & Malsch (2006), Sukumar & Tabarraei (2004) and Wachspress (1975).

The outline of the paper is as follows. In Section 2, we introduce the mathematical model. In Section 3, we present the formulation of the new VEM proposed here. In Section 4, we present the convergence analysis of the scheme. In Section 5, we confirm the theoretical results with numerical experiments. In Section 6, we offer final remarks and conclusions.

2. The mathematical model

Let us consider the steady diffusion problem for the scalar solution field u given by

$$-\mathrm{div}(\mathsf{K}\nabla u) = f \quad \text{in } \Omega, \tag{2.1}$$

$$u = g \quad \text{on } \Gamma, \tag{2.2}$$

where $\Omega \subset \mathbb{R}^2$ is the computational domain, Γ is the boundary of Ω, K is the diffusion tensor describing the material properties, f is the forcing term and g is the Dirichlet datum. For simplicity of exposition,

we will focus on the case of homogeneous Dirichlet boundary conditions, that is, $g = 0$. The more general case is a straightforward extension and will be considered for the numerical experiments in Section 5.

We assume the following:

(H1) Ω is a bounded, open, polygonal subset of $\mathbb{R}^2$;

(H2) the diffusion tensor $\mathsf{K} : \Omega \to \mathbb{R}^{2\times 2}$, is a 2×2, bounded, measurable and symmetric tensor. Moreover, we assume that K is *strongly elliptic*, that is, there exist two positive constants κ_* and κ^* such that for every $\mathbf{x} \in \Omega$ it holds

$$\kappa_* ||\mathbf{v}||^2 \leqslant \mathbf{v} \cdot \mathsf{K}(\mathbf{x})\mathbf{v} \leqslant \kappa^* ||\mathbf{v}||^2 \quad \forall \mathbf{v} \in \mathbb{R}^2, \tag{2.3}$$

where $||\mathbf{v}||$ is the usual Euclidean norm of the vector $\mathbf{v}$;

(H3) the function f belongs to $L^2(\Omega)$.

Throughout the paper, we will follow the usual notation for Sobolev spaces and norms (see, for example, Ciarlet, 1978). In particular, for a bounded and open domain $\mathcal{D}$, we will use $\|\cdot\|_{s,\mathcal{D}}$ and $|\cdot|_{s,\mathcal{D}}$ to denote the norm and the seminorm in the Sobolev space $H^s(\mathcal{D})$, while $(\cdot,\cdot)_{0,\mathcal{D}}$ will denote the $L^2(\mathcal{D})$ inner product. Often the subscript will be omitted when $\mathcal{D}$ is the computational domain Ω. Moreover, we represent the set of polynomials of degree *at most* j on P by $\mathbb{P}_j(\mathsf{P})$. Finally, $\pi_j^{\mathcal{D}}$ will denote the usual $L^2(\mathcal{D})$ projection onto $\mathbb{P}_j(\mathcal{D})$, $j \in \mathbb{N}$.

Let us now consider the functional space $H_0^1(\Omega) = \{v \in H^1(\Omega),\ v_{|\Gamma} = 0\}$. Problem (2.1–2.2) can be restated in variational form:

find $u \in H_0^1(\Omega)$ *such that*

$$\mathcal{A}(u, v) = (f, v) \quad \forall v \in H_0^1(\Omega), \tag{2.4}$$

where

$$\mathcal{A}(u, v) = \int_\Omega \mathsf{K}\nabla u \cdot \nabla v \, \mathrm{d}V \quad \text{and} \quad (f, v) = \int_\Omega fv \, \mathrm{d}V.$$

Under assumptions (H1)–(H3), the bilinear form $\mathcal{A}$ is continuous and coercive and the linear functional $(f, \cdot)$ is continuous, thus implying the well-posedness of problem (2.4), that is, existence and uniqueness of the weak solution (Grisvard, 1985).

3. The discrete model

Let $\{\Omega_h\}_h$ be a sequence of decompositions of Ω into elements P labelled by the mesh size parameter h. For the moment, we assume that each decomposition Ω_h is made of a finite number of *simple polygons*, that is, open, simply connected sets whose boundary is a nonintersecting line made of a finite number of straight line segments.

For every h, we construct a finite-dimensional space $V_h \subset H_0^1(\Omega)$, a bilinear form $\mathcal{A}_h : V_h \times V_h \to \mathbb{R}$ and a linear functional $(f_h, \cdot)_h : V_h \to \mathbb{R}$ such that the discrete problem

find $u_h \in V_h$ *such that*

$$\mathcal{A}_h(u_h, v_h) = (f_h, v_h)_h \quad \forall\, v_h \in V_h \tag{3.1}$$

has a unique solution u_h, and we have 'good' approximation properties. If $m \geqslant 1$ is the target degree of accuracy, and the solution u of (2.4) is smooth enough, we want to have

$$\|u - u_h\|_1 \leqslant Ch^m |u|_{m+1}, \tag{3.2}$$

where C is a positive constant independent of h.

3.1 *Local discrete spaces*

We denote a generic mesh vertex by v and its coordinate vector by $\mathbf{x}_\mathsf{v}$, a generic mesh edge by e and its length by $|\mathsf{e}|$, the area of polygon P by $|\mathsf{P}|$ and its boundary by $\partial\mathsf{P}$. The orientation of each edge e is reflected by its unit normal vector $\mathbf{n}_\mathsf{e}$, which is fixed once and for all. For any polygon P and any edge e of $\partial\mathsf{P}$, we define the unit normal vector $\mathbf{n}_{\mathsf{P},\mathsf{e}}$ that points out of P. We denote the set of mesh vertices by $\mathcal{V}$ and the set of mesh edges by $\mathcal{E}$.

We refer to the integer number $\alpha \geqslant 0$ as the *regularity index* and to the integer number $m \geqslant \alpha + 1$ as the *consistency index*. For any integer $s \geqslant 0$, we define the functional space

$$\mathbb{B}_s(\partial\mathsf{P}) := \{v \in L^2(\partial\mathsf{P}) \,:\, v_{|\mathsf{e}} \in \mathbb{P}_s(\mathsf{e})\ \forall \mathsf{e} \in \partial\mathsf{P}\}.$$

Now, let $\alpha_j := \max\{2(\alpha - j) + 1, m - j\}$ so that for example, $\alpha_0 := \max\{2\alpha + 1, m\}$ and $\alpha_1 := \max\{2\alpha - 1, m - 1\}$. We define the operator $\nabla^j v$ as the *collection of derivatives of order j* of the scalar function v, with the usual convention that the zeroth-order derivative coincides with the function. Thus, for example, it holds that $\nabla^0 v = v$, while $\nabla^1 v$ is the gradient of v, $\nabla^2 v$ is the Hessian, etc. For each polygonal cell P and any pair of indices (α, m) with $\alpha \geqslant 0$ and $m \geqslant \alpha + 1$, we consider the local finite element space

$$V_{h|\mathsf{P}} = \left\{ v \in H^{1+\alpha}(\mathsf{P}) \text{ with } \Delta^{1+\alpha} v \in \mathbb{P}_{m-2}(\mathsf{P}) \text{ and } \left.\frac{\partial^j v}{\partial n^j}\right|_{\partial\mathsf{P}} \in \mathbb{B}_{\alpha_j}(\partial\mathsf{P}) \text{ for } j = 0, \ldots, \alpha \right\}, \tag{3.3}$$

with the convention that $\mathbb{P}_{-1}(\mathsf{P}) = \{0\}$ and where $\Delta^{1+\alpha}$ represents the Laplace operator Δ applied $(1 + \alpha)$ times. Note that the conditions in (3.3) imply, in particular, that $\nabla^j v_{|\partial\mathsf{P}} \in C^0(\partial\mathsf{P})$.

Let us illustrate the meaning of this definition through a couple of examples. For $\alpha = 0$ and $m \geqslant 1$, we obtain the finite element spaces introduced in Beirão da Veiga *et al.* (2013), which allow for the formulation of a family of schemes that are equivalent to the arbitrary-order mimetic method in Beirão da Veiga *et al.* (2011b). In particular, for $m = 1$, we have the low-order nodal MFD method (Brezzi *et al.*, 2009). The functions that belong to these spaces are the solutions of the equation $\Delta v = p$ with $p \in \mathbb{P}_{m-2}(\mathsf{P})$ inside each polygonal cell P, and their trace on the boundary $\partial\mathsf{P}$ is a continuous piecewise polynomial of degree m. For $\alpha = 1$ and $m = 2$, we obtain the finite element space of functions in $H^2(\mathsf{P})$ that satisfy the following conditions:

- the trace on the boundary of P is continuous and on each edge is a polynomial of degree $\alpha_0 = 3$;
- the gradient on the boundary is continuous and on each edge the normal derivative is a polynomial of degree $\alpha_1 = 1$;
- inside P these functions satisfy the biharmonic equation $\Delta^2 v = p$ with $p \in \mathbb{R}$.

REMARK 3.1 For $\alpha = 0$ and $m = 1$ on triangles (the lowest-order-accurate lowest regular approximation that we can build) the VEM considered here coincides with the linear conforming finite element method.

However, for $\alpha = 0$ and $m > 1$, even on triangles, the virtual element schemes are no longer conforming finite elements as the internal degrees of freedom are not the same as those used in the higher-order conforming finite element approximation; cf. Beirão da Veiga *et al.* (2011b) and Beirão da Veiga & Manzini (2012). Moreover, for $\alpha > 0$ the method presented here does not correspond to any classical FEM method. Indeed, the construction of C^1 (or more regular) finite element spaces on unstructured meshes is much more complicated and needs to use either higher polynomial orders or subdivision of elements. In the special case of a rectangular mesh and $\alpha = 1, m = 3$, the method resembles the (tensor-product) Hermite element, but it is not the same scheme since the internal degrees of freedom are different.

REMARK 3.2 The local space $V_{h|\mathsf{P}}$ in (3.3) is virtual in the sense that we will not need to build it explicitly in order to implement the family of schemes proposed here.

3.2 *Local degrees of freedom*

We distinguish three kinds of degrees of freedom that are associated with each polygonal cell P:

- $\mathcal{V}^h_{\mathsf{P}}$: *vertex* degrees of freedom of P;
- $\mathcal{E}^h_{\mathsf{P}}$: *edge* degrees of freedom of P;
- $\mathcal{P}^h_{\mathsf{P}}$: *interior* degrees of freedom of P.

In Fig. 1, we depict some sample choices of degrees of freedom on a pentagonal element for $\alpha = 0, 1, 2$ and $m = \alpha + 1, \alpha + 2$.

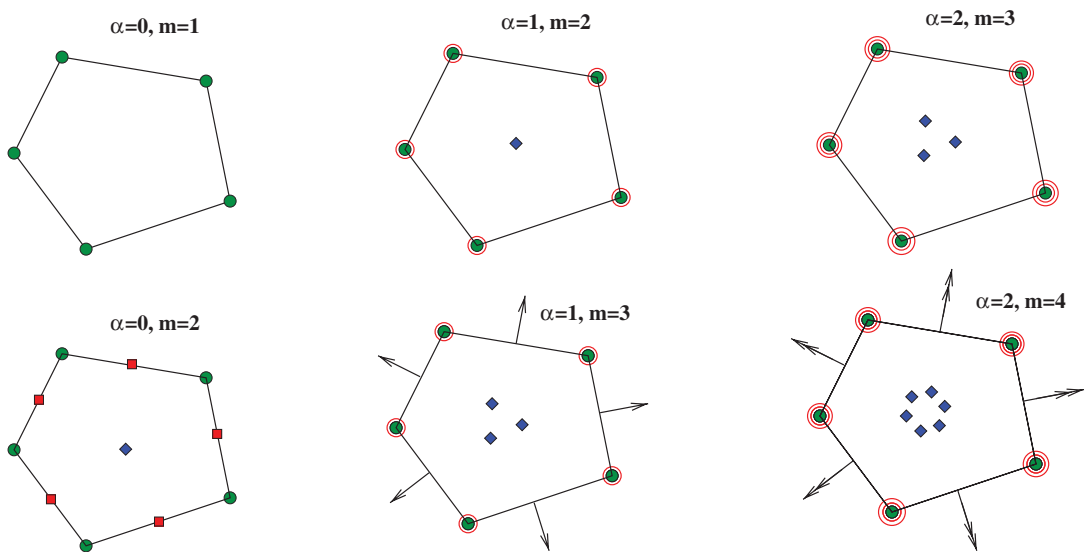

FIG. 1. Degrees of freedom for $\alpha = 0, 1, 2$ and $m = \alpha + 1, \alpha + 2$. The symbols shown in the plots represent vertex values (dot), vertex first-order derivatives (one circle), vertex first- and second-order derivatives (two circles), edge values (square), first-order normal derivatives (arrow), first- and second-order normal derivatives (double arrow).

Vertex degrees of freedom. The vertex degrees of freedom of a function v associated with the vertex v are the partial derivatives $\nabla^j v(\mathsf{v})$ for $j=0,1,\ldots,\alpha$ of degree up to α evaluated at $\mathbf{x}_\mathsf{v}$. For instance, for $\alpha=1$, we consider the value of $v(\mathbf{x}_\mathsf{v})$ and $\nabla v(\mathbf{x}_\mathsf{v})$ at each vertex v of $\partial\mathsf{P}$. For each mesh vertex, the total number of such degrees of freedom is given by $(\alpha+1)(\alpha+2)/2$.

Edge degrees of freedom. Let us consider a set of $\mathcal{N}_j^{\alpha,m}$ distinct nodes $\{\mathbf{x}_i^j\}_{i=1,\ldots,\mathcal{N}_j^{\alpha,m}}$ on the open edge e, where

$$\mathcal{N}_j^{\alpha,m}=\max(m-(\alpha+1)-(\alpha-j),0) \tag{3.4}$$

for $\alpha\geqslant 0$, $m\geqslant\alpha+1$ and $j=0,\ldots,\alpha$. These points can be uniformly spaced along e or chosen as the nodes of suitable integration rules like those provided by Gauss–Lobatto formulas; cf. Beirão da Veiga *et al.* (2011b). For each $j=0,\ldots,\alpha$, the edge degrees of freedom of a function v are given by the $\mathcal{N}_j^{\alpha,m}$ normal derivatives $\partial^j v(\mathbf{x}_k^j)/\partial n^j$ evaluated at these points (as usual, for $j=0$, we take the function value). For each edge e of $\partial\mathsf{P}$, the total number of such degrees of freedom is given by

$$\frac{(m-\alpha+\beta)(m-\alpha-1-\beta)}{2}+\beta,\quad \text{where } \beta=\max\{m-(2\alpha+1),0\}.$$

Note that when $m=\alpha+1$ there are no edge degrees of freedom, since, in such a case, formula (3.4) gives $\mathcal{N}_j^{\alpha,m}=0$ for all $j=0,\ldots,\alpha$.

Internal degrees of freedom. Let $\mathbf{s}=(s_1,s_2)$ denote a two-dimensional multi-index with the usual notation $|\mathbf{s}|:=s_1+s_2$ and $\mathbf{x}^\mathbf{s}=x_1^{s_1}x_2^{s_2}$ when $\mathbf{x}=(x_1,x_2)$. For $m>1$ we consider the set of $m(m-1)/2$ monomials

$$\mathcal{M}_{m-2}=\left\{\left(\frac{\mathbf{x}-\mathbf{x}_\mathsf{P}}{h_\mathsf{P}}\right)^\mathbf{s},\ |\mathbf{s}|\leqslant m-2\right\}, \tag{3.5}$$

which is a basis for $\mathbb{P}_{m-2}(\mathsf{P})$. The *internal degrees of freedom* of the function v are the moments:

$$\frac{1}{|\mathsf{P}|}\int_\mathsf{P} q(\mathbf{x})v(\mathbf{x})\,\mathrm{d}V\quad\forall q\in\mathcal{M}_{m-2}(\mathsf{P}).$$

The total number of internal degrees of freedom is $m(m-1)/2$.

The dimension $\mathcal{N}_\mathsf{P}^{\alpha,m}$ of the local space $V_{h|\mathsf{P}}$ equals the total number of degrees of freedom of $\mathcal{V}_\mathsf{P}^h$ plus $\mathcal{E}_\mathsf{P}^h$ plus $\mathcal{P}_\mathsf{P}^h$ and is given by

$$\mathcal{N}_\mathsf{P}^{\alpha,m}=N_\mathsf{P}^\mathcal{E}\left(\frac{(\alpha+1)(\alpha+2)}{2}+\frac{(m-\alpha)(m-\alpha-1)}{2}\right)+\frac{m(m-1)}{2}, \tag{3.6}$$

where $N_\mathsf{P}^\mathcal{E}$ is the number of edges of the polygon P. We still need to prove the unisolvence of the chosen degrees of freedom.

REMARK 3.3 The degrees of freedom $\mathcal{V}_\mathsf{P}^h$ plus $\mathcal{E}_\mathsf{P}^h$ uniquely determine a polynomial of degree α_0 on each edge e of P, which represents the function value, and α polynomials of degree α_j, $j=1,2,\ldots,\alpha$, each one of which represents the jth normal derivative along the edge. In other words, $\mathcal{V}_\mathsf{P}^h$ plus $\mathcal{E}_\mathsf{P}^h$ are equivalent to prescribing $\partial^j v/\partial n^j$ on $\partial\mathsf{P}$, for $j=0,1,\ldots,\alpha$. On the other hand, the degrees of freedom

$\mathcal{P}^h_{\mathsf{P}}$ are equivalent to prescribing $\pi^{\mathsf{P}}_{m-2}(v)$ in P. We recall that π^{P}_{m-2} is the projection operator, in the $L^2(\mathsf{P})$ norm, onto the space $\mathbb{P}_{m-2}(\mathsf{P})$.

For the space $V_{h|\mathsf{P}}$ and the degrees of freedom $\mathcal{V}^h_{\mathsf{P}}$ plus $\mathcal{E}^h_{\mathsf{P}}$ plus $\mathcal{P}^h_{\mathsf{P}}$ we have the following *unisolvence result*.

PROPOSITION 3.4 Let P be a simple polygon with $N^{\mathcal{E}}_{\mathsf{P}}$ edges, and let the space $V_{h|\mathsf{P}}$ be defined as in (3.3). The degrees of freedom $\mathcal{V}^h_{\mathsf{P}}$ plus $\mathcal{E}^h_{\mathsf{P}}$ plus $\mathcal{P}^h_{\mathsf{P}}$ are unisolvent for $V_{h|\mathsf{P}}$.

Proof. The present proof is similar to the analogous one in Beirão da Veiga *et al.* (2013). We present it for completeness. According to Remark 3.3, to prove the proposition it is enough to show that a function $v \in V_{h|\mathsf{P}}$ such that

$$\frac{\partial^j v}{\partial n^j} = 0 \quad \text{for } j = 0, 1, \ldots, \alpha, \text{ on } \partial\mathsf{P} \tag{3.7}$$

and

$$\pi^{\mathsf{P}}_{m-2}(v) = 0 \quad \text{in } \mathsf{P}, \tag{3.8}$$

is actually identically zero in P. In order to prove this, we show that $\Delta^{1+\alpha} v = 0$ in P (that joined with (3.7) gives $v \equiv 0$). To this end, we first solve, for every $q \in \mathbb{P}_{m-2}(\mathsf{P})$, the following auxiliary problem:

$$\begin{aligned} \sigma \Delta^{1+\alpha} w &= q \quad \text{in } \mathsf{P}, \\ \frac{\partial^j w}{\partial n^j} &= 0 \quad \text{on } \partial\mathsf{P} \quad \text{for } j \in [0, \alpha], \end{aligned} \tag{3.9}$$

where $\sigma = (-1)^{1+\alpha}$. This problem is reformulated in variational form as follows:

$$\textit{find } w \in H^{1+\alpha}_0(\mathsf{P}) \textit{ such that } \mathcal{B}_{\mathsf{P}}(w, v) = (q, v)_{0,\mathsf{P}} \quad \forall v \in H^{1+\alpha}_0(\mathsf{P}), \tag{3.10}$$

with $\mathcal{B}_{\mathsf{P}}$ denoting the elliptic bilinear form associated to the operator $\sigma \Delta^{1+\alpha}$ on P through the usual integration by parts. The solution of (3.9) can be written as $w = \sigma \Delta^{-1-\alpha}_{0,\mathsf{P}}(q)$, the latter symbol representing the inverse operator applied to the right-hand side function q.

Next, we consider the map R, from $\mathbb{P}_{m-2}(\mathsf{P})$ into itself, defined by

$$R(q) := \pi^{\mathsf{P}}_{m-2}(\sigma \Delta^{-1-\alpha}_{0,\mathsf{P}}(q)) \equiv \pi^{\mathsf{P}}_{m-2}(w). \tag{3.11}$$

We claim that R is an isomorphism. Indeed, from (3.11), the definition of π^{P}_{m-2}, and (3.10) we have, for every $q \in \mathbb{P}_{m-2}(\mathsf{P})$,

$$(R(q), q)_{0,\mathsf{P}} = (\pi^{\mathsf{P}}_{m-2}(\sigma \Delta^{-1-\alpha}_{0,\mathsf{P}}(q)), q)_{0,\mathsf{P}} = (\pi^{\mathsf{P}}_{m-2}(w), q)_{0,\mathsf{P}} = (w, q)_{0,\mathsf{P}} = \mathcal{B}_{\mathsf{P}}(w, w).$$

Since w is in $H^{1+\alpha}_0(\mathsf{P})$ we have then that

$$R(q) = 0 \Leftrightarrow \mathcal{B}_{\mathsf{P}}(w, w) = 0 \Leftrightarrow w = 0 \Leftrightarrow q = 0. \tag{3.12}$$

We note that, if $\partial^j v / \partial n^j = 0$ on $\partial\mathsf{P}$, $j = 0, \ldots, \alpha$, then

$$\pi^{\mathsf{P}}_{m-2}(v) = \pi_{m-2}(\sigma \Delta^{-1-\alpha}_{0,\mathsf{P}}(\sigma \Delta^{1+\alpha} v)) = R(\sigma \Delta^{1+\alpha} v).$$

Hence, $\pi^{\mathsf{P}}_{m-2}(v) = 0 \Longrightarrow R(\sigma \Delta^{1+\alpha} v) = 0 \Longrightarrow \sigma \Delta^{1+\alpha} v = 0$, and the proof is concluded. □

REMARK 3.5 We obtain a much better condition number of the stiffness matrix, and we also simplify its construction (see Section 3.4), by scaling the nodal degrees of freedom as follows. Let v be a vertex or an edge node of $\mathsf{P} \in \Omega_h$. We set

$$h_v = \max_{\{\mathsf{P}: v \in \partial \mathsf{P}\}} h_{\mathsf{P}}.$$

Then, we multiply all the degrees of freedom that are derivatives of order j in v by $(h_v)^j$.

3.3 *Construction of the finite element space V_h*

We can now design V_h, the *virtual element space* on the whole domain Ω. For every decomposition Ω_h of Ω into simple polygons P we first define the *space without boundary conditions*:

$$W_h = \{v \in H^{1+\alpha}(\Omega) \,:\, v_{|\mathsf{P}} \in V_{h|\mathsf{P}} \ \forall \mathsf{P} \in \Omega_h\}. \tag{3.13}$$

In agreement with the local choice of the degrees of freedom, in W_h we choose the following *degrees of freedom*:

- $\mathcal{V}^h$: the value of $\nabla^j v_h$, $j = 0, \ldots, \alpha$, at the vertices of $\mathcal{V}$;
- $\mathcal{E}^h$: the value of $\partial^j v_h / \partial n^j$ for $j = 0, \ldots, \alpha$ at the $\mathcal{N}_j^{\alpha,m}$ internal nodes of each edge of $\mathcal{E}$, where $\mathcal{N}_j^{\alpha,m}$ is defined in (3.4);
- $\mathcal{P}^h$: the value of the moments

$$\frac{1}{|\mathsf{P}|} \int_{\mathsf{P}} q(\mathbf{x}) v_h(\mathbf{x}) \, \mathrm{d}V \quad \forall q \in \mathcal{M}_{m-2}(\mathsf{P}), \ \ m \geqslant 2$$

  in each polygonal cell P, where the set $\mathcal{M}_{m-2}(\mathsf{P})$ is defined in (3.5).

Finally, the discrete space $V_h = W_h \cap H_0^1(\Omega)$ is given by

$$V_h = \{v \in H^{1+\alpha}(\Omega) \,:\, v_{|\mathsf{P}} \in V_{h|\mathsf{P}} \ \forall \mathsf{P} \in \Omega_h, \ v_{|\partial\Omega} = 0\}. \tag{3.14}$$

Note that the condition $v_h \in V_h$ implies $v_h = 0$ on the vertices and the edges of the boundary Γ. Therefore, the degrees of freedom of V_h are simply the ones introduced above, excluding the nodal degrees of freedom associated with the function values (but not with the derivatives) of the boundary vertices and edges. The dimension of V_h equals the total number of degrees of freedom for vertices, edges and elements. Proposition 3.4 implies that the global degrees of freedom are unisolvent for the global space V_h.

3.4 *Construction of $\mathcal{A}_h$*

We build the discrete bilinear form $\mathcal{A}_h$ by assembling the local bilinear forms $\mathcal{A}_{h,\mathsf{P}}$ in accordance with

$$\mathcal{A}_h(w_h, v_h) = \sum_{\mathsf{P} \in \Omega_h} \mathcal{A}_{h,\mathsf{P}}(w_h, v_h) \quad \forall w_h, v_h \in V_h. \tag{3.15}$$

The local bilinear forms $\mathcal{A}_{h,\mathsf{P}}$ are all *symmetric* and satisfy the following fundamental properties of *consistency* and *stability*.

- *Consistency:* for all h and for all P in Ω_h it holds

$$\mathcal{A}_{h,\mathsf{P}}(p, v_h) = \int_{\Omega} (\pi^{\mathsf{P}}_{m-1}(\mathsf{K}\nabla p)) \cdot \nabla v_h \, \mathrm{d}V \quad \forall p \in \mathbb{P}_m(\mathsf{P}), \ \ \forall v_h \in V_{h|\mathsf{P}}. \tag{3.16}$$

- *Stability*: there exist two positive constants α_* and α^*, independent of h and P, such that

$$\alpha_* \mathcal{A}_{\mathsf{P}}(v_h, v_h) \leqslant \mathcal{A}_{h,\mathsf{P}}(v_h, v_h) \leqslant \alpha^* \mathcal{A}_{\mathsf{P}}(v_h, v_h) \quad \forall v_h \in V_{h|\mathsf{P}}, \tag{3.17}$$

where the local bilinear form $\mathcal{A}_{\mathsf{P}}$ is defined as

$$\mathcal{A}_{\mathsf{P}}(w, v) = \int_{\mathsf{P}} \mathsf{K}\nabla w \cdot \nabla v \, \mathrm{d}V. \tag{3.18}$$

Note that in the present paper we consider a more general diffusion tensor K with respect to Beirão da Veiga *et al.* (2013), which is the reason for the modified consistency condition (3.16). However, in the case that $\mathsf{K}_{|\mathsf{P}}$ is constant, the projection operator π^{P}_{m-1} in (3.16) can be neglected, thus giving

$$\mathcal{A}_{h,\mathsf{P}}(p, v_h) = \mathcal{A}_{\mathsf{P}}(p, v_h) \quad \forall p \in \mathbb{P}_m(\mathsf{P}), \ \ \forall v_h \in V_{h|\mathsf{P}}.$$

The local degrees of freedom allow us to compute $\mathcal{A}_{h,\mathsf{P}}(p, v_h)$ exactly for any $p \in \mathbb{P}_m(\mathsf{P})$ and for any $v_h \in V_{h|\mathsf{P}}$. Indeed, let us assume (3.16) and integrate by parts:

$$\begin{aligned} \mathcal{A}_{h,\mathsf{P}}(p, v_h) &= \int_{\Omega} (\pi^{\mathsf{P}}_{m-1}(\mathsf{K}\nabla p)) \cdot \nabla v_h \, \mathrm{d}V \\ &= -\int_{\mathsf{P}} \operatorname{div}(\pi^{\mathsf{P}}_{m-1}(\mathsf{K}\nabla p)) v_h \, \mathrm{d}V + \int_{\partial\mathsf{P}} \mathbf{n}_{\mathsf{P}} \cdot (\pi^{\mathsf{P}}_{m-1}(\mathsf{K}\nabla p)) v_h \, \mathrm{d}S. \end{aligned} \tag{3.19}$$

Since $\operatorname{div}(\pi^{\mathsf{P}}_{m-1}(\mathsf{K}\nabla p)) \in \mathbb{P}_{m-2}(\mathsf{P})$, the first integral on the right-hand side of (3.19) can be expressed through the polynomial moments of v_h, and can thus be computed exactly by using its internal degrees of freedom. On the other hand, it holds that $\mathbf{n}_{\mathsf{P}} \cdot (\pi^{\mathsf{P}}_{m-1}(\mathsf{K}\nabla p)) \in \mathbb{P}_{m-1}(\mathsf{e})$ and $v_{h|\mathsf{e}} \in \mathbb{P}_{\alpha_0}(\mathsf{e})$ for all $\mathsf{e} \subset \partial\mathsf{P}$, and the second integral on the right-hand side of (3.19) can be computed exactly. Therefore, the right-hand side of (3.16) can be computed exactly without knowing v_h in the interior of P.

We also observe that, as a consequence of (3.17), the symmetry of the bilinear form $\mathcal{A}_{h,\mathsf{P}}$ and the continuity of $\mathcal{A}_{\mathsf{P}}$ in $H^1(\mathsf{P})$, it easily follows that (see Beirão da Veiga *et al.*, 2013 for the details)

$$\mathcal{A}_{h,\mathsf{P}}(v_h, w_h) \leqslant C|v_h|_{1,\mathsf{P}}|w_h|_{1,\mathsf{P}} \quad \forall v_h, w_h \in V_{h|\mathsf{P}}, \tag{3.20}$$

with the constant $C = C(\alpha^*, \kappa^*)$ independent of h.

REMARK 3.6 For all $p, q \in \mathbb{P}_m(\mathsf{P})$, from the definition of π^{P}_{m-1} and since $\nabla q \in \mathbb{P}_{m-1}(\mathsf{P})$, it follows that

$$\mathcal{A}_{h,\mathsf{P}}(p, q) = \int_{\Omega} (\pi^{\mathsf{P}}_{m-1}(\mathsf{K}\nabla p)) \cdot \nabla q \, \mathrm{d}V = \int_{\Omega} (\mathsf{K}\nabla p) \cdot \nabla q \, \mathrm{d}V = \mathcal{A}_{\mathsf{P}}(p, q).$$

Therefore, the bilinear form turns out to be exact when both entries are polynomials, even if K is not constant on the element P. Note that the above identity also implies that the consistency condition is compatible with the symmetry of $\mathcal{A}^{\mathsf{P}}_h$, since it gives $\mathcal{A}_{h,\mathsf{P}}(p, q) = \mathcal{A}_{h,\mathsf{P}}(q, p)$ for all $p, q \in \mathbb{P}_m(\mathsf{P})$.

We are left to show how to construct a computable $\mathcal{A}_h$ that satisfies (3.16) and (3.17). Different constructions are possible at this point. In this subsection we present the formal construction of the local bilinear forms that avoids matrix or index notation. Later on, in Section 4.3, we will show a more practical approach that directly addresses the implementation of the local stiffness matrix.

For any $\mathsf{P} \in \Omega_h$ and, for any sufficiently regular function φ, we set

$$\bar{\varphi} := \frac{1}{N_{\mathsf{P}}^{\mathcal{V}}} \sum_{i=1}^{N_{\mathsf{P}}^{\mathcal{V}}} \varphi(\mathbf{x}_{\mathsf{v}_i}), \tag{3.21}$$

where $\mathbf{x}_{\mathsf{v}_i}$ is the position vector of v_i, the ith vertex of $\partial\mathsf{P}$ in a local numbering system for i running from 1 to $N_{\mathsf{P}}^{\mathcal{V}}$.

Next, we define the operator $\Pi_m^{\mathsf{P}} : V_{h|\mathsf{P}} \longrightarrow \mathbb{P}_m(\mathsf{P}) \subset V_{h|\mathsf{P}}$ as the solution of

$$\begin{cases} \mathcal{A}_{\mathsf{P}}(\Pi_m^{\mathsf{P}}(v_h), q) = \displaystyle\int_{\Omega} (\pi_{m-1}^{\mathsf{P}}(\mathsf{K}\nabla q)) \cdot \nabla v_h \, \mathrm{d}V \quad \forall q \in \mathbb{P}_m(\mathsf{P}), \\ \overline{\Pi_m^{\mathsf{P}}(v_h)} = \bar{v}_h, \end{cases} \tag{3.22}$$

for all $v_h \in V_{h|\mathsf{P}}$, where $\bar{v}_h$ is the cell average of v_h over cell P. System (3.22) implies that

$$\Pi_m^{\mathsf{P}}(p) = p \quad \forall p \in \mathbb{P}_m(\mathsf{P}), \tag{3.23}$$

since the first equation will tell us that p and $\Pi_m^{\mathsf{P}}(p)$ have the same gradient, and the second equation takes care of the constant part.

At this point, choosing $\mathcal{A}_{h,\mathsf{P}}(u, v) = \mathcal{A}_{\mathsf{P}}(\Pi_m^{\mathsf{P}}(u), \Pi_m^{\mathsf{P}}(v))$ for any couple of functions u and v would ensure property (3.16), but (3.17) in general would not be verified. We need to add a term able to ensure (3.17). Let $S^{\mathsf{P}}(u, v)$ be *any symmetric and positive definite* bilinear form such that

$$c_0 \mathcal{A}_{\mathsf{P}}(v, v) \leqslant S^{\mathsf{P}}(v, v) \leqslant c_1 \mathcal{A}_{\mathsf{P}}(v, v) \quad \forall v \in V_{h|\mathsf{P}} \quad \text{with } \Pi_m^{\mathsf{P}}(v) = 0 \tag{3.24}$$

for some positive constants c_0 and c_1 independent of P and h_{P} using the same bilinear form $\mathcal{A}_{\mathsf{P}}$ defined in (3.18).

Then, we set

$$\mathcal{A}_{h,\mathsf{P}}(u, v) = \mathcal{A}_{\mathsf{P}}(\Pi_m^{\mathsf{P}}(u), \Pi_m^{\mathsf{P}}(v)) + S^{\mathsf{P}}(u - \Pi_m^{\mathsf{P}}(u), v - \Pi_m^{\mathsf{P}}(v)) \tag{3.25}$$

for any couple of functions u and v in $V_{h|\mathsf{P}}$. The following lemma can be verified immediately.

LEMMA 3.7 The bilinear form (3.25) satisfies the consistency property (3.16) and the stability property (3.17).

In general, the choice of the bilinear form S^{P} would depend on the problem and on the degrees of freedom. From (3.24) it is clear that S^{P} must scale like $\mathcal{A}_{\mathsf{P}}$ on the kernel of Π_m^{P}. For each element $\mathsf{P} \in \Omega_h$, we denote by χ_i, $i = 1, \ldots, \mathcal{N}_{\mathsf{P}}^{\alpha,m}$ the operator that associates the ith local degree of freedom

$\chi_i(\varphi)$ with each smooth enough function φ. Then, by choosing the canonical basis $\varphi_1, \ldots, \varphi_{\mathcal{N}_\mathsf{P}^{\alpha,m}}$ as

$$\chi_i(\varphi_j) = \delta_{ij}, \quad i,j = 1, \ldots, \mathcal{N}_\mathsf{P}^{\alpha,m}, \tag{3.26}$$

(with $\mathcal{N}_\mathsf{P}^{\alpha,m}$ defined in (3.6)), the local stiffness matrix is given by

$$\mathcal{A}_{h,\mathsf{P}}(\varphi_i, \varphi_j) = \mathcal{A}_\mathsf{P}(\Pi_m^\mathsf{P}(\varphi_i), \Pi_m^\mathsf{P}(\varphi_j)) + S^\mathsf{P}(\varphi_i - \Pi_m^\mathsf{P}(\varphi_i), \varphi_j - \Pi_m^\mathsf{P}(\varphi_j)). \tag{3.27}$$

In our case it is easy to check that there must hold $\mathcal{A}_\mathsf{P}(\varphi_i, \varphi_i) \simeq |\varphi_i|^2_{1,\mathsf{P}} \simeq 1$ for each 'reasonable polygon' (for example, any polygon satisfying the mesh assumptions that will be discussed in Section 4). This property is true for all $i = 1, 2, \ldots, \mathcal{N}_\mathsf{P}^{\alpha,m}$ since we properly scaled the local degrees of freedom; see (3.5) and Remark 3.5. Therefore, a simple choice for S^P that satisfies (3.24) is given by

$$S^\mathsf{P}(\varphi_i - \Pi_m^\mathsf{P}(\varphi_i), \varphi_j - \Pi_m^\mathsf{P}(\varphi_j)) = \sum_{r=1}^{\mathcal{N}_\mathsf{P}^{\alpha,m}} \chi_r(\varphi_i - \Pi_m^\mathsf{P}(\varphi_i))\chi_r(\varphi_j - \Pi_m^\mathsf{P}(\varphi_j)).$$

3.5 *Construction of the loading term*

We first consider the case $m \geqslant 2$, and define f_h on each element P as the $L^2(\mathsf{P})$ projection of f onto the space $\mathbb{P}_{m-2}$, that is,

$$f_h = \pi_{m-2}^\mathsf{P}(f) \quad \text{on each } \mathsf{P} \in \Omega_h.$$

The loading term can be transformed as

$$(f_h, v_h)_h = \sum_{\mathsf{P}\in\Omega_h} \int_\mathsf{P} f_h v_h \, \mathrm{d}V \equiv \sum_{\mathsf{P}\in\Omega_h} \int_\mathsf{P} \pi_{m-2}^\mathsf{P}(f) v_h \, \mathrm{d}V = \sum_{\mathsf{P}\in\Omega_h} \int_\mathsf{P} f \pi_{m-2}^\mathsf{P}(v_h) \, \mathrm{d}V,$$

where the last identity follows from the fact that v_h and $\pi_{m-2}^\mathsf{P}(v_h)$ have the same internal moments. Thus, the right-hand side of (3.1) can be computed exactly by using the degrees of freedom of the functions in V_h that represent the internal moments. For $m = 1$, we approximate f by the piecewise constant whose restriction to P is $\pi_0^\mathsf{P}(f)$, and we define the right-hand side of (3.1) by

$$(f_h, v_h) = \sum_{\mathsf{P}\in\Omega_h} \int_\mathsf{P} \pi_0^\mathsf{P}(f) \bar{v}_h \, \mathrm{d}V = \sum_{\mathsf{P}\in\Omega_h} |\mathsf{P}| \pi_0^\mathsf{P}(f) \bar{v}_h, \tag{3.28}$$

where $\bar{v}_h$ is given by (3.21).

4. Convergence analysis

In this section we carry out the convergence analysis of the method.

4.1 *Mesh regularity assumption*

We will make use of the following regularity assumption on the mesh.

Assumption 4.1 (Mesh assumption) There exists a real number $\gamma > 0$ such that, for all h, each element P in Ω_h is star shaped with respect to a ball of radius at least γh_P, where h_P is the diameter of P.

Moreover, there exists a real number $\gamma' > 0$ such that, for all h and for each element P in Ω_h, the distance between any two vertices of P is at least $\gamma' h_{\mathsf{P}}$.

REMARK 4.2 The above mesh conditions can be relaxed. We refer the interested reader to Beirão da Veiga *et al.* (2013) for a thorough discussion concerning this issue.

We now consider the following discrete approximations of the solution u. For each element $\mathsf{P} \in \Omega_h$, we extend the set of operators χ_i for $i = 1, \ldots, \mathcal{N}_{\mathsf{P}}^{\alpha,m}$, which are defined on the functions of $\mathcal{V}_{\mathsf{P}}^h$, to any sufficiently regular function φ. When applied to φ, these operators return the local degrees of freedom $\chi_i(\varphi)$ associated with cell P. It follows that for any such function φ there exists a unique element φ^{I} of $V_{h|\mathsf{P}}$ such that

$$\chi_i(\varphi - \varphi^{\mathrm{I}}) = 0, \quad i = 1, \ldots, \mathcal{N}_{\mathsf{P}}^{\alpha,m}. \tag{4.1}$$

In the following, we will make use of the interpolant $u^{\mathrm{I}} \in V_h$ of the exact solution u.

LEMMA 4.3 Let u be a function in $H^{s+1}(\mathsf{P})$ for any integer $s \geqslant \alpha + 1$ and u^{I} its interpolant in $V_{h|\mathsf{P}}$ defined through the local degrees of freedom $\chi_i(\varphi)$ associated with cell P. Let u_π be the L^2 projection of u on the space of (discontinuous) functions that are piecewise polynomials of degree m on the mesh Ω_h. Under Assumption 4.1 on the mesh regularity, the following approximation result holds:

$$|u - u_\pi|_{1,\mathsf{P}} + |u - u^{\mathrm{I}}|_{1,\mathsf{P}} \lesssim h_{\mathsf{P}}^s |u|_{s+1,\mathsf{P}}. \tag{4.2}$$

Proof. The lemma is a consequence of the Scott–Dupont approximation theory on star-shaped domains; see, for example, Brenner & Scott (2008). □

4.2 *Convergence theorem*

The following convergence theorem holds.

THEOREM 4.4 Let the consistency and stability assumptions (3.16–3.17) on the method, and the mesh assumptions considered above, hold. Then, the discrete problem

find $u_h \in V_h$ *such that*

$$\mathcal{A}_h(u_h, v_h) = (f_h, v_h)_h \quad \forall\, v_h \in V_h \tag{4.3}$$

has a unique solution.

Moreover, let the tensor $K_{|}\mathsf{P}$ be in $W^{s,\infty}$ for all $\mathsf{P} \in \Omega_h$. Then, if the solution u belongs to $H^{1+\alpha}(\Omega)$, it holds that

$$|u - u_h|_1 \leqslant C h^s |u|_{s+1} \tag{4.4}$$

for all $1 + \alpha \leqslant s \leqslant m$, where C is a constant independent of h.

Proof. Existence and uniqueness of the solution of (4.3) is a consequence of (3.17) and of the coercivity of $\mathcal{A}$. To ease the notation, we will use the symbol $\lesssim$ to indicate bounds up to a constant that is independent of h. Setting $\delta_h := u_h - u^{\mathrm{I}}$, using (4.3), (3.15), and adding and subtracting u_π (the L^2

projection of u defined in Lemma 4.3), it follows that

$$\begin{aligned} k_\star\alpha_*|\delta_h|_1^2 &\leqslant \alpha_*\mathcal{A}(\delta_h,\delta_h)\\ &\leqslant \mathcal{A}_h(\delta_h,\delta_h)\\ &= \mathcal{A}_h(u_h,\delta_h) - \mathcal{A}_h(u^{\mathrm{I}},\delta_h)\\ &= (f_h,\delta_h)_h - \sum_{\mathsf{P}\in\Omega_h}\mathcal{A}_{h,\mathsf{P}}(u^{\mathrm{I}},\delta_h)\\ &= (f_h,\delta_h)_h - \sum_{\mathsf{P}\in\Omega_h}(\mathcal{A}_{h,\mathsf{P}}(u^{\mathrm{I}}-u_\pi,\delta_h)+\mathcal{A}_{h,\mathsf{P}}(u_\pi,\delta_h)). \end{aligned} \tag{4.5}$$

From the above equation, first using (3.16) and then by some simple manipulation, we obtain

$$\begin{aligned} |\delta_h|_1^2 &\lesssim (f_h,\delta_h)_h - \sum_{\mathsf{P}\in\Omega_h}(\mathcal{A}_{h,\mathsf{P}}(u^{\mathrm{I}}-u_\pi,\delta_h)+\mathcal{A}_{\mathsf{P}}(u_\pi,\delta_h)+T_1^{\mathsf{P}})\\ &= (f_h,\delta_h)_h - \sum_{\mathsf{P}\in\Omega_h}(\mathcal{A}_{h,\mathsf{P}}(u^{\mathrm{I}}-u_\pi,\delta_h)+\mathcal{A}_{\mathsf{P}}(u_\pi-u,\delta_h)+T_1^{\mathsf{P}})-\mathcal{A}(u,\delta_h), \end{aligned} \tag{4.6}$$

where we introduced the term

$$T_1^{\mathsf{P}} = \int_{\mathsf{P}}(\pi_{m-1}^{\mathsf{P}} - I)(\mathsf{K}\nabla u_\pi)\cdot\nabla\delta_h. \tag{4.7}$$

Now, recalling (2.4), the above bound yields

$$\begin{aligned} |\delta_h|_1^2 &\lesssim (f_h,\delta_h)_h - \sum_{\mathsf{P}\in\Omega_h}(\mathcal{A}_{h,\mathsf{P}}(u^{\mathrm{I}}-u_\pi,\delta_h)+\mathcal{A}_{\mathsf{P}}(u_\pi-u,\delta_h)+T_1^{\mathsf{P}})-(f,\delta_h)\\ &= T_f - \sum_{\mathsf{P}\in\Omega_h}(T_1^{\mathsf{P}}+T_2^{\mathsf{P}}+T_3^{\mathsf{P}}), \end{aligned} \tag{4.8}$$

where the terms

$$T_f = (f_h,\delta_h)_h - (f,\delta_h), \tag{4.9}$$

$$T_2^{\mathsf{P}} = \mathcal{A}_{h,\mathsf{P}}(u^{\mathrm{I}}-u_\pi,\delta_h), \tag{4.10}$$

$$T_3^{\mathsf{P}} = \mathcal{A}_{\mathsf{P}}(u_\pi-u,\delta_h). \tag{4.11}$$

We need to bound the three terms above. By assuming that f is sufficiently regular and using the same argument as in Beirão da Veiga *et al.* (2013,?), we obtain the following approximation estimate:

$$|(f_h,\delta_h)_h - (f,\delta_h)| \lesssim h^s\left(\sum_{\mathsf{P}\in\Omega_h}|f|_{s-1,\mathsf{P}}^2\right)^{1/2}|\delta_h|_1. \tag{4.12}$$

We thus obtain the inequality

$$|T_f| \lesssim h^s|u|_{s+1}|\delta_h|_1. \tag{4.13}$$

By a triangle inequality and using the continuity of both $\mathcal{A}_{\mathsf{P}}$ and $\mathcal{A}_{h,\mathsf{P}}$ (see (3.20)), we obtain

$$|T_2^{\mathsf{P}}| + |T_3^{\mathsf{P}}| \lesssim (|u - u_\pi|_{1,\mathsf{P}} + |u - u^{\mathrm{I}}|_{1,\mathsf{P}})|\delta_h|_{1,\mathsf{P}}. \tag{4.14}$$

Combining (4.14) with the approximation result of Lemma 4.3 gives the estimate

$$|T_2^{\mathsf{P}}| + |T_3^{\mathsf{P}}| \lesssim h_{\mathsf{P}}^s |u|_{s+1,\mathsf{P}} |\delta_h|_{1,\mathsf{P}}. \tag{4.15}$$

We finally bound the terms T_1^{P}. We first note that by the Cauchy–Schwarz inequality we have

$$|T_1^{\mathsf{P}}| \leqslant ||(\pi_{m-1}^{\mathsf{P}} - I)(\mathsf{K}\nabla u_\pi)||_{0,\mathsf{P}} |\delta_h|_{1,\mathsf{P}}. \tag{4.16}$$

By the triangle inequality and recalling the definition of π_{m-1}^{P} we obtain

$$\begin{aligned} ||(\pi_{m-1}^{\mathsf{P}} - I)(\mathsf{K}\nabla u_\pi)||_{0,\mathsf{P}} &\leqslant ||(\pi_{m-1}^{\mathsf{P}} - I)(\mathsf{K}\nabla u)||_{0,\mathsf{P}} + ||(\pi_{m-1}^{\mathsf{P}} - I)(\mathsf{K}\nabla (u - u_\pi))||_{0,\mathsf{P}} \\ &\leqslant ||(\pi_{m-1}^{\mathsf{P}} - I)(\mathsf{K}\nabla u)||_{0,\mathsf{P}} + ||\mathsf{K}\nabla (u - u_\pi)||_{0,\mathsf{P}}. \end{aligned} \tag{4.17}$$

By using a standard approximation estimate on polygons and recalling the hypothesis of regularity on K, the last inequality in (4.7) implies that

$$||(\pi_{m-1}^{\mathsf{P}} - I)(\mathsf{K}\nabla u_\pi)||_{0,\mathsf{P}} \lesssim h^s |u|_{s+1,\mathsf{P}} + |u - u_\pi|_{1,\mathsf{P}} \lesssim h^s |u|_{s+1,\mathsf{P}}. \tag{4.18}$$

We consider (4.16–4.18) and we have

$$|T_1^{\mathsf{P}}| \lesssim h^s |u|_{s+1,\mathsf{P}} |\delta_h|_{1,\mathsf{P}}. \tag{4.19}$$

A bound for $|\delta_h|_1$ follows easily by combining (4.8) with (4.13), (4.15) and (4.19). Finally, the result is obtained by a triangle inequality and from Lemma 4.3. □

REMARK 4.5 We note that the interpolated field u^{I} can also be defined in a different way, for example, by using local integrals in accordance with the classical Clément approximation. In such a case, the elementwise locality of the approximation estimates is lost, but the regularity requirement for the solution u is relaxed to $u \in H^\alpha(\Omega)$.

The regularity requirement on u appearing in (4.4) is not realistic when K is discontinuous across the edges of the mesh Ω_h. Indeed, in such a case a discrete space V_h with C^1 or higher regularity is not the best choice. Nevertheless, the schemes considered herein can be easily adapted in order to make use of a less regular space V_h across *selected vertices and edges* of the mesh. To this purpose, we consider the same degrees of freedom for each element P, but those associated with first- or higher-order derivatives at the nodes of the chosen edges or at the selected vertices are no longer single valued and may take different values when referred to different elements. This strategy requires only the assembly of the global stiffness matrix to be modified, while the construction of the local element matrices remains unchanged. The resulting discrete space V_h will show C^0 regularity only across the selected edges.

4.3 *Implementation of the local stiffness matrices*

In this section, we show an algebraic construction of the local stiffness matrix associated to $\mathcal{A}_{h,\mathsf{P}}$, $\mathsf{P} \in \Omega_h$. The final formula for the stiffness matrix, which is suitable for direct interpretation, is similar to the matrix formulas found in the mimetic literature.

We refer the interested reader to Beirão da Veiga & Manzini (2012) for a deeper investigation of the connection with the MFD scheme.

Given $\mathsf{P} \in \Omega_h$, we build an elemental stiffness matrix M_P such that

$$\mathcal{A}_{h,\mathsf{P}}(w_{h,\mathsf{P}}, v_{h,\mathsf{P}}) = \underline{w}_{h,\mathsf{P}}^{\mathrm{T}} \mathsf{M}_\mathsf{P} \underline{v}_{h,\mathsf{P}} \quad \forall w_{h,\mathsf{P}},\ v_{h,\mathsf{P}} \in \mathcal{V}_\mathsf{P}^h,$$

where the vectors $\underline{w}_{h,\mathsf{P}}$ and $\underline{v}_{h,\mathsf{P}}$ represent the local degrees of freedom of $w_{h,\mathsf{P}}$ and $v_{h,\mathsf{P}}$. The global stiffness matrix is then obtained by a standard finite-element-like assembly procedure.

To this purpose, we first construct two matrices N_P and R_P that satisfy an algebraic form of consistency condition (3.16), that is, that are such that $\mathsf{M}_\mathsf{P}\mathsf{N}_\mathsf{P} = \mathsf{R}_\mathsf{P}$ and $\mathsf{N}_\mathsf{P}^{\mathrm{T}}\mathsf{R}_\mathsf{P}$ is a symmetric and nonnegative-definite matrix. Let p_i be the ith element of the basis $\mathcal{M}_m(\mathsf{P})$ for the polynomial space $\mathbb{P}_m(\mathsf{P})$. The index i runs from 1 to $n := (m+1)(m+2)/2$ and suitably renumbers the monomials forming $\mathcal{M}_m(\mathsf{P})$; for example,

$$p_1(x,y) = 1,$$
$$p_2(x,y) = (x - x_\mathsf{P})/h_\mathsf{P}, \quad p_3(x,y) = (y - y_\mathsf{P})/h_\mathsf{P}, \quad \text{etc.}$$

Taking $\mathcal{N}_\mathsf{P}^{\alpha,m}$ degrees of freedom of $\mathcal{V}_\mathsf{P}^h$ in accordance with (4.1), we define the matrix $\mathsf{N}_\mathsf{P} \in \mathbb{R}^{\mathcal{N}_\mathsf{P}^{\alpha,m} \times n}$ by

$$(\mathsf{N}_\mathsf{P})_{ij} = \chi_i(p_j).$$

The columns of matrix R_P, which belongs to $\mathbb{R}^{\mathcal{N}_\mathsf{P}^{\alpha,m} \times n}$, represent the right-hand side of the consistency condition given by (3.16) applied to the polynomials $\{p_1, p_2, \ldots, p_n\}$. Let $\varepsilon_{h,\mathsf{P}}^i$ indicate the unique function in $\mathcal{V}_\mathsf{P}^h$ such that $\chi_j(\varepsilon_{h,\mathsf{P}}^i) = \delta_{ij}$, $i,j = 1,2,\ldots,\mathcal{N}_\mathsf{P}^{\alpha,m}$. Matrix R_P takes the form

$$(\mathsf{R}_\mathsf{P})_{ij} = \int_\Omega (\pi_{m-1}^\mathsf{P}(\mathsf{K}\nabla p_j)) \cdot \nabla \varepsilon_{h,\mathsf{P}}^i \, \mathrm{d}V$$

for $i = 1,\ldots,\mathcal{N}_\mathsf{P}^{\alpha,m}$ and $j = 1,\ldots,n$, which is computable thanks to the observations in Section 3.4.

From the definitions above it is easy to show that $\mathsf{M}_\mathsf{P}\mathsf{N}_\mathsf{P} = \mathsf{R}_\mathsf{P}$, which is the matrix form of the consistency condition (3.16). Furthermore, a straightforward calculation shows that

$$(\mathsf{N}_\mathsf{P}^{\mathrm{T}}\mathsf{R}_\mathsf{P})_{ij} = \int_\mathsf{P} \mathsf{K}\nabla p_i \cdot \nabla p_j \, \mathrm{d}V, \tag{4.20}$$

that is, $\mathsf{N}_\mathsf{P}^{\mathrm{T}}\mathsf{R}_\mathsf{P}$ is symmetric and semipositive definite. Let K_P (not to be confused with the diffusivity tensor K) be the square symmetric matrix that represents the bilinear form $\mathcal{A}_h$ restricted to the space $\mathbb{P}_m(\mathsf{P})$ so that

$$\mathsf{K}_\mathsf{P} = \mathsf{N}_\mathsf{P}^{\mathrm{T}}\mathsf{M}_\mathsf{P}\mathsf{N}_\mathsf{P} = \mathsf{N}_\mathsf{P}^{\mathrm{T}}\mathsf{R}_\mathsf{P}. \tag{4.21}$$

Matrix K_P has the block-diagonal form

$$\mathsf{K}_\mathsf{P} = \begin{pmatrix} 0 & \mathbf{0} \\ \mathbf{0} & \hat{\mathsf{K}}_\mathsf{P} \end{pmatrix},$$

where $\hat{\mathsf{K}}_\mathsf{P} \in \mathbb{R}^{(n-1)\times(n-1)}$ is a strictly positive-definite matrix. More precisely, matrix $\hat{\mathsf{K}}_\mathsf{P}$ is the strictly positive-definite matrix that is given by (4.20) if we do not consider the row $i = 1$ and the column $j = 1$,

that is, the constant polynomial $p_1(x, y) = 1$. Let $\mathsf{K}_\mathsf{P}^\dagger \in \mathbb{R}^{n\times n}$ be the pseudo-inverse of matrix K_P, which we define as

$$\mathsf{K}_\mathsf{P}^\dagger = \begin{pmatrix} 0 & \mathbf{0} \\ \mathbf{0} & \hat{\mathsf{K}}_\mathsf{P}^{-1} \end{pmatrix}.$$

Let us now consider the matrix

$$\Pi_\mathsf{P} = \mathsf{N}_\mathsf{P}\mathsf{K}_\mathsf{P}^\dagger\mathsf{R}_\mathsf{P}^\mathrm{T}, \tag{4.22}$$

which is indicated, with a small abuse of notation, by using the same symbol 'Π' of the corresponding operator defined in (3.22).

In accordance with (3.25) and (3.27), the local stiffness matrix of the VEM on cell P is given by

$$\mathsf{M}_\mathsf{P} = \mathsf{R}_\mathsf{P}\mathsf{K}_\mathsf{P}^\dagger\mathsf{R}_\mathsf{P}^\mathrm{T} + \eta(\mathsf{I} - \Pi_\mathsf{P})^\mathrm{T}\mathsf{P}_\mathsf{P}(\mathsf{I} - \Pi_\mathsf{P}), \tag{4.23}$$

where the positive scalar η is equal to the trace of $\mathsf{R}_\mathsf{P}\mathsf{K}_\mathsf{P}^\dagger\mathsf{R}_\mathsf{P}^\mathrm{T}$, I is the (properly sized) identity matrix, and P_P is a symmetric and positive-semidefinite matrix that does not scale with h. An effective choice for P_P is given by

$$\mathsf{P}_\mathsf{P} = \mathsf{I} - \mathsf{N}_\mathsf{P}(\mathsf{N}_\mathsf{P}^\mathrm{T}\mathsf{N}_\mathsf{P})^{-1}\mathsf{N}_\mathsf{P}^\mathrm{T}. \tag{4.24}$$

Using (4.24) in (4.23) (and a few straightforward manipulations) yields

$$\mathsf{M}_\mathsf{P} = \mathsf{R}_\mathsf{P}\mathsf{K}_\mathsf{P}^\dagger\mathsf{R}_\mathsf{P}^\mathrm{T} + \eta\mathsf{P}_\mathsf{P}, \tag{4.25}$$

which is a well-known formula for the mimetic schemes. Matrix M_P in (4.25) is the formula for the local stiffness matrix that we used to implement, the numerical schemes considered in Section 5. The bilinear form associated with matrix M_P satisfies both the consistency and stability conditions. Indeed, matrix P_P is the projector to the orthogonal complement of the space spanned by the columns of matrix N_P and the product $\mathsf{P}_\mathsf{P}\mathsf{N}_\mathsf{P}$ is zero. Therefore, also due to (4.21), we immediately have the consistency condition (3.16) in the matrix form $\mathsf{M}_\mathsf{P}\mathsf{N}_\mathsf{P} = \mathsf{R}_\mathsf{P}$. The purpose of the second matrix in (4.23) is only to guarantee the coercivity (up to the correct kernel) of the system, and, thus, the stability property of (3.17). This latter property can be checked by following the same (standard) arguments that are commonly used in the mimetic literature.

REMARK 4.6 We note that the first matrix on the right-hand side of (4.23) corresponds to the first term on the right-hand side of (3.27). Instead, the other two matrices in (4.23) and (3.27) may be different, but serve the same purpose of guaranteeing the stability.

5. Numerical experiments

The numerical experiments presented in this section are designed to confirm the *a priori* analysis developed in the previous section in a general setting. In particular, when we use a method corresponding to the pair (α, m), the numerical solution is expected to behave like an m-order-accurate approximation of the exact solution in the H^1 norm, assuming that this latter is at least $H^{1+\alpha}$ regular. Since the discrete solution u_h is unknown inside the element, we evaluate the H^1 norm of the error through the

mesh-dependent norm

$$\|v_h\|_{1,h}^2 = \sum_{\mathsf{P}\in\Omega_h} \|v_h\|_{1,h,\mathsf{P}}^2, \tag{5.1}$$

where each term $\|v_h\|_{1,h,\mathsf{P}}$ is a local approximation of the energy seminorm of v_h. For $m \geqslant 2$, this local contribution reads as

$$\begin{aligned}\|v_h\|_{1,h,\mathsf{P}}^2 = &\sum_{\mathsf{e}\in\partial\mathsf{P}} h_{\mathsf{P}} |v_h|_{H^1(\mathsf{e})}^2 + \sum_{j=1}^{\alpha} \sum_{\mathsf{e}\in\partial\mathsf{P}} h_{\mathsf{P}}^{2j-1} \|\partial_n^j v_h\|_{L^2(\mathsf{e})}^2 \\ &+ \left(\frac{1}{|\mathsf{P}|}\int_{\mathsf{P}} v_h \,\mathrm{d}V - \bar{v}_{h,\mathsf{P}}\right)^2 + \sum_{j=1}^{m-2} \sum_{q\in\mathcal{M}_j(\mathsf{P})} \left(\frac{1}{|\mathsf{P}|}\int_{\mathsf{P}} v_h q \,\mathrm{d}V\right)^2,\end{aligned} \tag{5.2}$$

where $\bar{v}_{h,\mathsf{P}}$ is the arithmetic mean of the values that v_h takes at the $N_{\mathsf{P}}^{\mathcal{V}}$ vertices of the element P (here denoted by v_{v}), that is,

$$\bar{v}_{h,\mathsf{P}} = \frac{1}{N_{\mathsf{P}}^{\mathcal{V}}} \sum_{\mathsf{v}\in\partial\mathsf{P}} v_{\mathsf{v}}. \tag{5.3}$$

For $m = 1$, the last two summation terms in (5.2) must be neglected. It is easy to check that the kernel of the seminorm (5.2) is given by the constant functions, and that this seminorm scales like the H^1 seminorm. Therefore, norm $\|\cdot\|_{1,h}$ represents an H^1-type discrete norm. Recalling Theorem 4.4, we therefore expect that, under the same hypotheses, the rate of convergence measured by norm (5.1) will satisfy

$$\|u_h - u\|_{1,h,\mathsf{P}} \leqslant Ch^m |u|_{m+1},$$

as holds for the H^1 norm.

We solve the diffusion problem (2.1–2.2) on the domain $\Omega = [0,1]\times[0,1]$ with Dirichlet conditions assigned on all of the domain boundary Γ. The right-hand side f and the boundary function g are determined in accordance with the exact solution

$$u(x,y) = x\sin(2\pi x)\sin(2\pi y) + x^3y^2, \tag{5.4}$$

and the diffusion tensor

$$\mathsf{K}(x,y) = \begin{pmatrix} 1+y^2 & -xy \\ -xy & 1+x^2 \end{pmatrix}. \tag{5.5}$$

The performance of these new numerical methods is investigated by evaluating the rate of convergence on three families of refined meshes. The second mesh in each family is shown in Fig. 2 and the data of the refined meshes are given in Tables 1–3. In these tables, the columns labelled N_{P}, N_{e} and N_{v} report the number of mesh cells, edges and vertices, respectively; #dofs is the number of degrees of freedom and h is the mesh-size parameter.

Let us briefly describe the construction of these mesh families. The meshes in $\mathcal{M}_1$ are built by dualization of a regular triangular mesh after a smooth coordinate transformation. This kind of mesh is rather common in the mimetic literature; see, for example, Beirão da Veiga *et al.* (2009b). To this

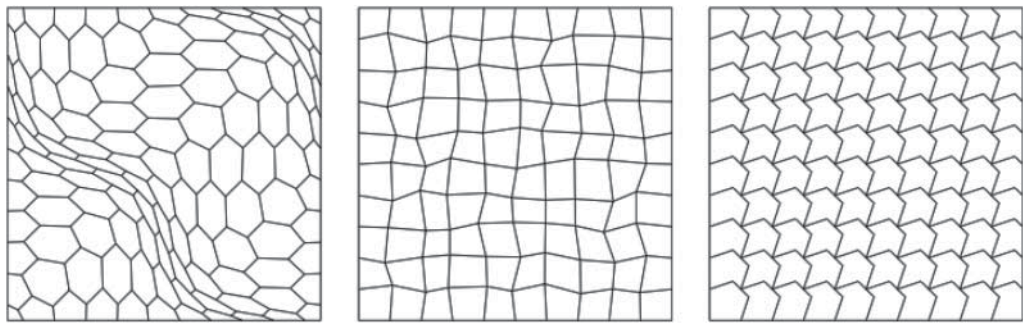

FIG. 2. Poisson problem on the square domain $[0,1] \times [0,1]$; from left to right: the mainly hexagonal mesh ($\mathcal{M}_1$), the mesh of randomized quadrilaterals ($\mathcal{M}_2$) and the nonconvex mesh corresponding to the second refinement level ($\mathcal{M}_3$).

TABLE 1 *Mesh data for the sequence $\mathcal{M}_1$ of meshes with mainly hexagonal cells; l is the refinement level, N_P is the number of cells, N_e is the number of edges, N_v is the number of vertices, #dofs is the number of degrees of freedom, h is the mesh size*

l	N_P	N_e	N_v	#dofs	h
1	36	125	90	251	3.405×10^{-1}
2	121	400	280	801	2.008×10^{-1}
3	441	1400	960	2801	1.071×10^{-1}
4	1681	5200	3520	10401	5.422×10^{-2}
5	6561	20000	13440	40001	2.719×10^{-2}
6	25921	78400	52480	156801	1.361×10^{-2}

TABLE 2 *Mesh data for the sequence $\mathcal{M}_2$ of randomized quadrilateral meshes; l is the refinement level, N_P is the number of cells, N_e is the number of edges, N_v is the number of vertices, #dofs is the number of degrees of freedom, h is the mesh size*

l	N_P	N_e	N_v	#dofs	h
1	25	60	36	121	3.311×10^{-1}
2	100	220	121	441	1.865×10^{-1}
3	400	840	441	1681	9.412×10^{-2}
4	1600	3280	1681	6561	4.693×10^{-2}
5	6400	12960	6561	25921	2.389×10^{-2}
6	25600	51520	25921	103041	1.221×10^{-2}

purpose, we remap the position $(\hat{x}, \hat{y})$ of the nodes of a uniform partition by the smooth coordinate transformation

$$\begin{aligned} x &= \hat{x} + \left(\frac{1}{10}\right) \sin(2\pi\hat{x}) \sin(2\pi\hat{y}), \\ y &= \hat{y} + \left(\frac{1}{10}\right) \sin(2\pi\hat{x}) \sin(2\pi\hat{y}). \end{aligned} \tag{5.6}$$

TABLE 3 *Mesh data for the sequence $\mathcal{M}_3$ of meshes with nonconvex cells; l is the refinement level, N_P is the number of cells, N_e is the number of edges, N_v is the number of vertices, #dofs is the number of degrees of freedom, h is the mesh size*

l	N_P	N_e	N_v	#dofs	h
1	25	120	96	241	2.915×10^{-1}
2	100	440	341	881	1.458×10^{-1}
3	400	1680	1281	3361	7.289×10^{-2}
4	1600	6560	4961	13121	3.644×10^{-2}
5	6400	25920	19521	51841	1.822×10^{-2}
6	25600	103040	77441	206081	9.111×10^{-3}

The meshes in $\mathcal{M}_1$ are built from the 'primal' mesh at level l by splitting each quadrilateral cell into two triangles and connecting the barycentres of adjacent triangular cells by a straight segment. The mesh construction is carried out at the boundary Γ by connecting the barycentres of the triangular cells close to Γ to the midpoints of the boundary edges and these latters to the boundary vertices of the 'primal' mesh. The leftmost plot of Fig. 2 shows the second refinement mesh of $\mathcal{M}_1$, which is built from an initial 10×10 regular partition.

The meshes in $\mathcal{M}_2$ are built by randomly perturbing an underlying uniform partition of the domain Ω formed by square-shaped elements. Since the randomization is carried out independently at every mesh refinement, there is no mesh regularization effect in the process as it occurs, for example, when a quadrilateral is split into four subcells by joining the midpoints of opposite edges. The middle plot of Fig. 2 shows the second refinement mesh of $\mathcal{M}_2$, which is built from an initial 10×10 regular partition.

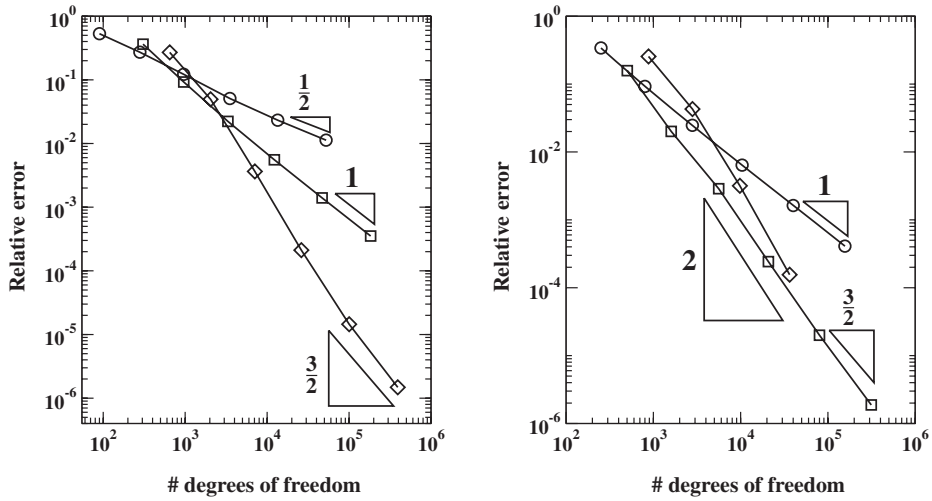

FIG. 3. Poisson problem on the square domain $[0, 1] \times [0, 1]$ with variable permeability using the mesh family $\mathcal{M}_1$ (mainly hexagonal meshes); the error curves correspond to the schemes labelled (α, m) with $\alpha = 0$ (circles), $\alpha = 1$ (squares), $\alpha = 2$ (diamonds) and $m = \alpha + 1$ (left plot), $m = \alpha + 2$ (right plot); the expected rates are of order $\mathcal{O}(N^{-\nu})$ with $\nu = m/2$ (since $N \approx h^{-2}$); exact slopes corresponding to ν are shown in each plot for comparison.

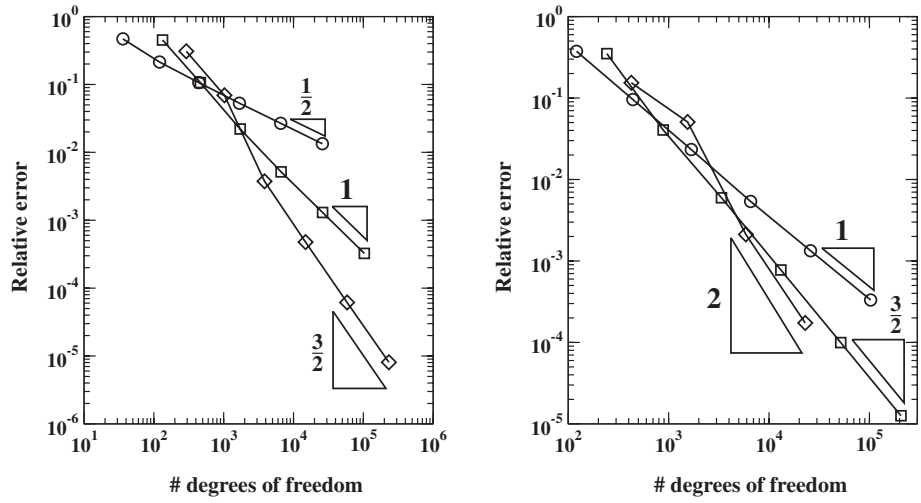

FIG. 4. Poisson problem on the square domain $[0,1] \times [0,1]$ with variable permeability using the mesh family $\mathcal{M}_2$ (randomized quadrilateral meshes); the error curves correspond to the schemes labelled (α, m) with $\alpha = 0$ (circles), $\alpha = 1$ (squares), $\alpha = 2$ (diamonds) and $m = \alpha + 1$ (left plot), $m = \alpha + 2$ (right plot); the expected rates are of order $\mathcal{O}(N^{-\nu})$ with $\nu = m/2$ (since $N \approx h^{-2}$); exact slopes corresponding to ν are shown in each plot for comparison.

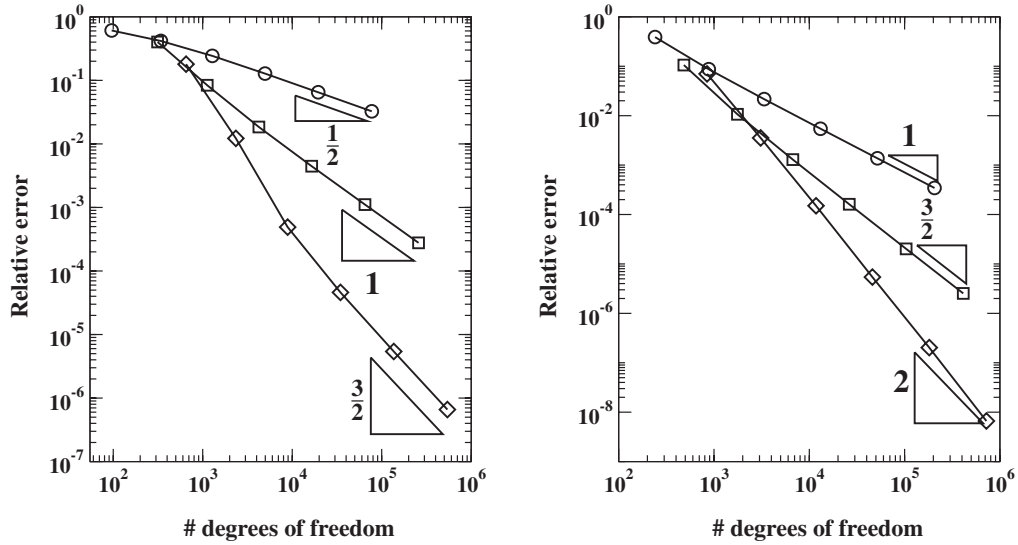

FIG. 5. Poisson problem on the square domain $[0,1] \times [0,1]$ with variable permeability using the mesh family $\mathcal{M}_3$ (nonconvex polygon meshes); the error curves correspond to the schemes labelled (α, m) with $\alpha = 0$ (circles), $\alpha = 1$ (squares), $\alpha = 2$ (diamonds) and $m = \alpha + 1$ (left plot), $m = \alpha + 2$ (right plot); the expected rates are of order $\mathcal{O}(N^{-\nu})$ with $\nu = m/2$ (since $N \approx h^{-2}$); exact slopes corresponding to ν are shown in each plot for comparison.

As shown in the rightmost plot of Fig. 2, a nonconvex mesh of $\mathcal{M}_3$ is made of a regular pattern of octagonal cells, which are built by adding a mesh vertex at each edge midpoint of an underlying square mesh. This additional vertex is then translated by a fixed displacement vector when the original position lies in the interior of the computational domain. The rightmost plot of Fig. 2 shows the second refinement mesh of $\mathcal{M}_3$, which is built from an initial 10×10 regular partition.

The numerical results are shown in Figs 3–5 for mesh families $\mathcal{M}_1$, $\mathcal{M}_2$ and $\mathcal{M}_3$, respectively. In each figure, we show the error curves for the numerical approximation that are obtained by applying the virtual element schemes corresponding to the pair of indices (α, m) with $\alpha = 0, 1, 2$ and $m = \alpha + 1$ (left plots) and $m = \alpha + 2$ (right plots); see the captions for more details. The relative errors, which are measured by using the norm defined in (5.1), are plotted against N, the total number of degrees of freedom. The convergence rate on each mesh sequence is reflected by the slope of the corresponding error curve, and is expected to be of order $\mathcal{O}(N^{-m/2})$ asymptotically, since $N \approx h^{-2}$. In each plot, we show, for comparison, the theoretical slope and we also indicate the exponent. All these plots essentially confirm the good behaviour of the schemes that we propose in this paper.

6. Conclusions

In this work, we proposed and analysed a VEM that is suitable for the numerical approximation of second-order diffusion problems with variable coefficients and provides arbitrary regular discrete solutions. The numerical approximation can be of arbitrary order, the optimality being dependent on the regularity of the exact solution. The numerical results confirm the effectiveness of the approach.

As pointed out in Section 1 and remarked upon throughout the paper, the possibility of building such methods quite easily is one of the major properties of the VEM and, in this respect, this work is intended as a first contribution to the virtual finite element literature. Following the idea presented here opens a wide range of applications, such as, for example, easier discretization of higher-order problems, direct calculation of derived quantities (such as fluxes, strains, stresses), anisotropic error estimation based on the Hessian of the solution, better eigenvalue approximation, numerical treatment of the stream-function formulation of the Stokes problem, etc.

Funding

This work was partially supported by the National Nuclear Security Administration of the U.S. Department of Energy at Los Alamos National Laboratory under Contract No. DE-AC52-06NA25396 and the Department Of Energy Office of Science Advanced Scientific Computing Research (ASCR) Program in Applied Mathematics (to G.M.).

References

Argyris, J. H., Fried, I. & Scharpf, D. W. (1968) The TUBA family of plate elements for the matrix displacement method. *Aeronaut. J. R. Aeronaut. Soc.*, **72**, 701–709.

Beirão da Veiga, L. (2008) A residual based error estimator for the mimetic finite difference method. *Numer. Math.*, **108**, 387–406.

Beirão da Veiga, L. (2010) A mimetic discretization method for linear elasticity. *Math. Model. Numer. Anal.*, **44**, 231–250.

Beirão da Veiga, L., Brezzi, F., Cangiani, A., Manzini, G., Marini, L. D. & Russo, A. (2013) Basic principles of virtual element methods. *Math. Models Methods Appl. Sci.*, **23**, 119–214.

Beirão da Veiga, L., Brezzi, F. & Marini, L. D. (2013) Virtual elements for linear elasticity problems. *SIAM J. Num. Anal.*, **81**, 794–812.

Beirão da Veiga, L., Gyrya, V., Lipnikov, K. & Manzini, G. (2009a) Mimetic finite difference method for the Stokes problem on polygonal meshes. *J. Comput. Phys.*, **228**, 7215–7232.

Beirão da Veiga, L., Lipnikov, K. & Manzini, G. (2009b) Convergence analysis of the high-order mimetic finite difference method. *Numer. Math.*, **113**, 325–356.

Beirão da Veiga, L., Lipnikov, K. & Manzini, G. (2011b) Arbitrary-order nodal mimetic discretizations of elliptic problems on polygonal meshes. *SIAM J. Numer. Anal.*, **49**, 1737–1760.

Beirão da Veiga, L. & Manzini, G. (2008) An *a posteriori* error estimator for the mimetic finite difference approximation of elliptic problems. *Int. J. Numer. Meth. Eng.*, **76**, 1696–1723.

Beirão da Veiga, L. & Manzini, G. (2012) The mimetic finite difference method and the virtual element method for elliptic problems with arbitrary regularity. Technical Report (Preprint IMATI 2012), IMATI-CNR.

Bell, K. (1969) A refined triangular plate bending finite element. *Int. J. Numer. Meth. Eng.*, **1**, 101–122.

Belytschko, T., Lu, Y. Y. & Gu, L. (1994) Element-free Galerkin methods. *Int. J. Numer. Meth. Eng.*, **37**, 229–256. Available at http://dx.doi.org/10.1002/nme.1620370205.

Benson, D. J., Bazilevs, Y., De Luycker, E., Hsu, M.-C., Scott, M., Hughes, T. J. R. & Belytschko, T. (2010) A generalized finite element formulation for arbitrary basis functions: from isogeometric analysis to xfem. *Int. J. Numer. Meth. Eng.*, **83**, 765–785. Available at http://dx.doi.org/10.1002/nme.2864.

Brenner, S. C. & Scott, L. R. (2008) *The Mathematical Theory of Finite Element Methods*, 3rd edn. Texts in Applied Mathematics, vol. 15. New York: Springer.

Brezzi, F., Buffa, A. & Lipnikov, K. (2009) Mimetic finite differences for elliptic problems. *Math. Model. Numer. Anal.*, **43**, 277–295.

Brezzi, F., Lipnikov, K. & Shashkov, M. (2005a) Convergence of the mimetic finite difference method for diffusion problems on polyhedral meshes. *SIAM J. Numer. Anal.*, **43**, 1872–1896. ISSN 0036-1429.

Brezzi, F., Lipnikov, K. & Simoncini, V. (2005b) A family of mimetic finite difference methods on polygonal and polyhedral meshes. *Math. Models Methods Appl. Sci.*, **15**, 1533–1551. ISSN 0218-2025.

Brezzi, F. & Marini, L. D. (2013) Virtual element method for plate bending problems. *Comput. Methods Appl. Mech. Engrg.*, **253**, 455–462.

Cangiani, A. & Manzini, G. (2008) Flux reconstruction and pressure post-processing in mimetic finite difference methods. *Comput. Methods Appl. Mech. Eng.*, **197**, 933–945. (doi:10.1016/j.cma.2007.09.019)

Cangiani, A., Manzini, G. & Russo, A. (2009) Convergence analysis of the mimetic finite difference method for elliptic problems. *SIAM J. Numer. Anal.*, **47**, 2612–2637.

Ciarlet, P. G. (1978) *The Finite Element Method for Elliptic Problems*. Amsterdam: North-Holland.

Clough, R. W. & Tocher, J. L. (1965) Finite element stiffness matrices for analysis of plates in bending. *Proceedings of the Conference of Matrix Methods in Structural Mechanics*, Wright–Patterson AFB, Ohio.

Cottrell, J. A., Hughes, T. J. R. & Bazilevs, Y. (2009) *Isogeometric Analysis. Towards Integration of CAD and FEA*. New York: Wiley.

Cueto, E., Sukumar, N., Calvo, B., Martínez, M., Cegoñino, J. & Doblaré, M. (2003) Overview and recent advances in natural neighbour Galerkin methods. *Arch. Comput. Meth. Eng.*, **10**, 307–384. Available at http://dx.doi.org/10.1007/BF02736253.

de Boor, C. (2001) *A Practical Guide to Splines*. Berlin: Springer.

Fries, T.-P. & Belytschko, T. (2010) The extended/generalized finite element method: An overview of the method and its applications. *Int. J. Numer. Meth. Eng.*, **84**, 253–304. Available at http://dx.doi.org/10.1002/nme.2914.

Grisvard, P. (1985) *Elliptic Problems in Nonsmooth Domains*. Monographs and Studies in Mathematics, vol. 24. Boston: Pitman.

Lipnikov, K., Manzini, G. & Svyatskiy, D. (2011) Analysis of the monotonicity conditions in the mimetic finite difference method for elliptic problems. *J. Comput. Phys.*, **230**, 2620–2642. (doi:10.1006/j.jcp.2010.12.039)

Mousavi, S. & Sukumar, N. (2011) Numerical integration of polynomials and discontinuous functions on irregular convex polygons and polyhedrons. *Comput. Mech.*, **47**, 535–554. Available at http://dx.doi.org/10.1007/s00466-010-0562-5.

Schumaker, L. L. (2007) *Spline Functions: Basic Theory*, 3rd edn. Cambridge, UK: Cambridge University Press.

SUKUMAR, N. & MALSCH, E. (2006) Recent advances in the construction of polygonal finite element interpolants. *Archives of Computational Methods in Engineering*, **13**, 129–163. Available at http://dx.doi.org/10.1007/BF02905933.

SUKUMAR, N. & TABARRAEI, A. (2004) Conforming polygonal finite elements. *Int. J. Numer. Meth. Eng.*, **61**, 2045–2066.

WACHSPRESS, E. (1975) *A Rational Finite Element Basis*. New York: Academic Press.